0026-895X/09/7605-1082–1093$20.00
MOLECULAR PHARMACOLOGY
Copyright © 2009 The American Society for Pharmacology and Experimental Therapeutics
Mol Pharmacol 76:1082–1093, 2009

Vol. 76, No. 5
60160/3527407
Printed in U.S.A.

Caveolin-1 and Lipid Microdomains Regulate G_s Trafficking and Attenuate G_s/Adenylyl Cyclase Signaling

John A. Allen, Jiang Z. Yu, Rahul H. Dave, Anushree Bhatnagar, Bryan L. Roth, and Mark M. Rasenick

Departments of Physiology & Biophysics (J.A.A., J.Z.Y., R.H.D., M.M.R.) and Psychiatry (M.M.R.), University of Illinois at Chicago, College of Medicine, Chicago, Illinois; Lerner Research Institute, Cleveland Clinic Foundation, Cleveland, Ohio (A.B.); and Department of Pharmacology, University of North Carolina School of Medicine, Chapel Hill, North Carolina (J.A.A., B.L.R.)

Received August 6, 2009; accepted August 18, 2009

ABSTRACT

Lipid rafts and caveolae are specialized membrane microdomains implicated in regulating G protein-coupled receptor signaling cascades. Previous studies have suggested that rafts/caveolae may regulate β-adrenergic receptor/$G\alpha_s$ signaling, but underlying molecular mechanisms are largely undefined. Using a simplified model system in C6 glioma cells, this study disrupts rafts/caveolae using both pharmacological and genetic approaches to test whether caveolin-1 and lipid microdomains regulate G_s trafficking and signaling. Lipid rafts/caveolae were disrupted in C6 cells by either short-term cholesterol chelation using methyl-β-cyclodextrin or by stable knockdown of caveolin-1 and -2 by RNA interference. In imaging studies examining $G\alpha_s$-GFP during signaling, stimulation with the βAR agonist isoproterenol resulted in internalization of $G\alpha_s$-GFP; however, this trafficking was blocked by methyl-β-cyclodextrin or by caveolin knockdown. Caveolin knockdown significantly decreased $G\alpha_s$ localization in detergent insoluble lipid raft/caveolae membrane fractions, suggesting that caveolin localizes a portion of $G\alpha_s$ to these membrane microdomains. Methyl-β-cyclodextrin or caveolin knockdown significantly increased isoproterenol or thyrotropin-stimulated cAMP accumulation. Furthermore, forskolin- and aluminum tetrafluoride-stimulated adenylyl cyclase activity was significantly increased by caveolin knockdown in cells or in brain membranes obtained from caveolin-1 knockout mice, indicating that caveolin attenuates signaling at the level of $G\alpha_s$/adenylyl cyclase and distal to GPCRs. Taken together, these results demonstrate that caveolin-1 and lipid microdomains exert a major effect on $G\alpha_s$ trafficking and signaling. It is suggested that lipid rafts/caveolae are sites that remove $G\alpha_s$ from membrane signaling cascades and caveolins might dampen globally $G\alpha_s$/adenylyl cyclase/cAMP signaling.

Lipid rafts and caveolae are specialized membrane microdomains defined by their cholesterol- and sphingomyelin-rich nature, enrichment in glycosyl-phosphatidylinositolanchored proteins, cytoskeletal association, and their resistance to detergent extraction (Brown, 2006). Lipid rafts and caveolae selectively partition and organize proteins and lipids in membranes, and they have been implicated in the regulation of a variety of cellular functions. These include exo- and endocytosis, membrane scaffolding, control of cholesterol homeostasis, and transmembrane signal transduction. A growing body of evidence indicates lipid rafts/caveolae regulate many G protein-coupled receptor (GPCR) signaling cascades by differentially partitioning GPCRs, heterotrimeric G proteins, and their various effectors in membrane microdomains (for reviews, see Allen et al., 2007; Patel et al., 2008). In addition to acting as organizing centers for signaling molecules, both lipid rafts and caveolae/caveolins can facilitate clathrin-independent endocytosis (Le Roy and Wrana, 2005; Rajendran and Si-

This work was supported by the National Institutes of Health National Institute of Mental Health [Grants R01-MH78200, R01-MH39595, R01-MH61887]; National Institutes of Health National Institute on Drug Abuse [Grant R21-DA20568]; National Institutes of Health National Heart, Lung, and Blood Institute [Grant T32-HL07692]; National Institutes of Health National Institute of Child Health & Human Development [Grant T32-HD040127]; and the UNC Neurodevelopmental Disorders Research Center.

The study has been previously presented in preliminary form: Allen JA, Yu JZ, Bhatnagar A, Roth BB, and Rasenick MM (2006) Agonist induced internalization of G alpha s regulates adenylyl cyclase (Abstract). *FASEB J* **20:** A694; and Rasenick MM (2007) Regulation of G protein signaling by cytoskeletal components and membrane microdomains. Experimental Biology; April 28–May 2, 2007; Washington DC.

Article, publication date, and citation information can be found at http://molpharm.aspetjournals.org.

doi:10.1124/mol.109.060160.

ABBREVIATIONS: GPCR, G protein-coupled receptor; RNAi, RNA interference; GFP, green fluorescent protein; DMEM, Dulbecco's modified Eagle's medium; TSH, thyrotropin ; TSHR, thyrotropin receptor; DTT, dithiothreitol; BF, buoyant fraction; HF, heavy fraction; PBS, phosphate-buffered saline; PAGE, polyacrylamide gel electrophoresis; IBMX, 3-isobutyl-1-methylxanthine; AC VI, adenylyl cyclase type 6; AC, adenylyl cyclase; WT, wild-type; AR, adrenergic receptor; PTX, pertussis toxin.

mons, 2005) and thereby might modulate signal transduction by influencing trafficking of signaling proteins.

Caveolins are multifunctional scaffolding proteins that are essential for forming caveolae and recruiting proteins into these membrane microdomain invaginations (Cohen et al., 2004). Although there are three caveolin gene products, caveolae functions are dependent on caveolin-1, because caveolin-1 knockout mice do not form caveolae (Drab et al., 2001; Cohen et al., 2004) and expression of caveolin-1 results in de novo formation of caveolae (Fra et al., 1995). Caveolins may differentially regulate GPCR signaling by scaffolding and partitioning different receptors, G proteins and their effectors in caveolae. For example, stable knockdown of caveolin-1 in C6 glioma cells alters the signaling of only select $G\alpha_q$-coupled GPCRs, as caveolin knockdown abolishes signaling through 5-HT_{2A} and P2Y receptors, whereas thrombin signaling through Par1 is unaffected (Bhatnagar et al., 2004). By contrast, the signaling of $G\alpha_q$-coupled mGluR1/5 receptors is attenuated by caveolin-1 in human embryonic kidney 293 cells or cortical neurons (Francesconi et al., 2009). Therefore, caveolins and caveolae differentially influence GPCRs and can either promote or inhibit their signaling cascades.

The heterotrimeric G protein $G\alpha_s$ allosterically activates adenylyl cyclase resulting in cAMP production during GPCR signaling events. Several previous studies have demonstrated that $G\alpha_s$ and subtypes of adenylyl cyclase are localized and enriched in lipid rafts/caveolae in various tissues, including cardiomyocytes (Rybin et al., 2000; Head et al., 2005), endothelial cells (Oh and Schnitzer, 2001), and C6 glioma cells (Toki et al., 1999; Fagan et al., 2000), and this localization might modulate $G\alpha_s$-coupled GPCR signaling.

Numerous studies investigating the fate of activated $G\alpha_s$ have indicated that the G protein can undergo agonist-induced intracellular redistribution, and this redistribution can involve either a release from membranes and translocation into the cytosol/cytoplasm or endocytosis (internalization) (Rasenick et al., 1984; Rodbell, 1985; Ransnas et al., 1989; Levis and Bourne, 1992; Wedegaertner et al., 1996; Yu and Rasenick, 2002; Hynes et al., 2004); however, the intracellular fate, functional impact, and putative signaling of internalized $G\alpha_s$ is poorly understood (Marrari et al., 2007). Our recent studies of $G\alpha_s$ trafficking using a functional $G\alpha_s$-GFP fusion protein determined activation of $G\alpha_s$ results in its rapid internalization (Yu and Rasenick, 2002), which increases microtubule dynamics (Yu et al., 2009). $G\alpha_s$ internalization is dependent on lipid raft/caveolae domains (Allen et al., 2005). In addition, $G\alpha_s$ localization in lipid rafts/caveolae seems dynamic and may also be dependent on the actin and microtubule cytoskeletons. βAR stimulation of C6 cells increases $G\alpha_s$ partitioning into rafts/caveolae (Allen et al., 2005), whereas treatment with various antidepressant drugs or microtubule/actin depolymerizing drugs results in removal of $G\alpha_s$ from the microdomains (Donati and Rasenick, 2005; Head et al., 2006). How the partitioning of $G\alpha_s$ in lipid rafts/caveolae and trafficking of $G\alpha_s$ through those structures influences $G\alpha_s$ signaling remains unclear.

In this report, experiments test the hypothesis that caveolae/lipid rafts regulate $G\alpha_s$ trafficking and $G\alpha_s$/adenylyl cyclase signaling. We report that agonist-induced internalization of $G\alpha_s$-GFP during signaling is prevented by disrupting lipid rafts/caveolae through cholesterol chelation or by stable caveolin knockdown in C6 glioma cells. Disruption of lipid rafts/caveolae significantly increased $G\alpha_s$/adenylyl cyclase signaling induced by GPCR activation or direct $G\alpha_s$ activation in C6 cells and in brain tissue isolated from caveolin-1 knockout mice. These findings indicate that lipid rafts/caveolae and caveolin-1 exert a major effect on $G\alpha_s$ trafficking and signaling. These results further suggest that lipid rafts/caveolae represent plasma membrane microdomains in which $G\alpha_s$/adenylyl cyclase signaling is attenuated and may represent a portal for the regulation of cAMP signaling.

Materials and Methods

Caveolin-1 Knockout Mice. Caveolin-1 knockout mice are a whole-animal knockout of caveolin-1 and -2 (Razani et al., 2001) bred onto a C57/BL6 line obtained from The Jackson Laboratory (Bar Harbor, ME) and were colony maintained as heterozygote sibling breeding pairs. Just after weaning, 3-week-old offspring were ear-tagged and genotype-confirmed by polymerase chain reaction. Ten- to 12-week-old male wild-type and knockout littermate pairs were euthanized by decapitation, and striatum was immediately microdissected from whole brain. Crude striatal membranes were prepared from both isolated striatal hemispheres by homogenization of tissue in a sucrose-Tris buffer (50 mM Tris, 0.32M sucrose, 5 mM $MgCl_2$, 1 mM EGTA, and 1× protease inhibitors (Complete PI, Roche), pH 7.4) with the use of a Polytron homogenizer (Kinematica, Littau-Lucerne, Switzerland). The brain homogenates were centrifuged at 1000*g* for 15 min, the supernatant was reserved (S1), the pellet was resuspended in sucrose-Tris, and centrifugation was repeated. The second supernatant (S2) was combined with S1 and centrifuged at 30,000*g* for 20 min. The resulting membrane pellet was resuspended in 50 mM Tris, 1 mM EGTA, and 5 mM $MgCl_2$, and protein concentration was determined by the Bradford method (Bradford, 1976). Membranes separated into aliquots were frozen on dry ice and stored at −80 C° until use. Ten micrograms of striatal membranes were analyzed for adenylyl cyclase activity (described under *Adenylyl Cyclase Activity Assays*). All animals were maintained in accordance with the University of North Carolina's Institutional Animal Use and Care Committee Protocol and all procedures and euthanization adhered to standards in accordance with the PHS Welfare Act.

Cell Culture and Transfections. Wild-type C6 glioma cells were obtained from the American Type Culture Collection. C6 cells in which caveolin-1 is stably knocked-down by RNAi (Cav-1 RNAi) were prepared as described previously (Bhatnagar et al., 2004). These cells contain endogenous β-adrenergic receptors. C6 cells or Cav-1 RNAi cells were cultured in DMEM containing 4.5 g/l glucose, 10% calf serum supplemented with iron (HyClone, Logan, UT), 1% penicillin and streptomycin, and 1 mM sodium pyruvate and were maintained in 10% CO_2 at 37°C. Cav-1 RNAi cells were maintained in selection media containing normal DMEM (as above) supplemented with 0.6 μg/ml G418 (Geneticin; Invitrogen, Carlsbad, CA), to maintain selection of only stable RNAi clones. The $G\alpha_s$-GFP fusion protein has been described previously (Yu and Rasenick, 2002). For live-cell imaging, cells were seeded into 35-mm glass-bottomed dishes (Delta T Vision; Thermo Fisher Scientific, Waltham, MA). Cells were grown to 70% confluence and were cotransfected for 5 h with $G\alpha_s$-GFP (0.5 μg/dish), $G\beta_1$ (0.25 μg/dish), and $G\gamma_2$ (0.25 μg/dish), using a ratio of 1:5 DNA/SuperFect transfection reagent (QIAGEN, Valencia, CA). Twenty-four hours after $G\alpha_s$-GFP transfection, cells were used for imaging experiments. It is notable that in Cav-1 RNAi cells, unlike the parent C6 cells, $G\alpha_s$-GFP exhibited poor membrane localization. After a series of plasmid titrations, it was determined that coexpression of $G\beta_1$ and $G\gamma_2$ increased $G\alpha_s$-GFP localization at the plasma membrane in the caveolin knockdown cells. The involvement of $G\beta\gamma$ in targeting $G\alpha_s$ to the plasma membrane is well documented (Evanko et al., 2001; Marrari et al., 2007); coexpression of the complete heterotrimer presumably promotes

membrane targeting of $G\alpha_s$-GFP in the Cav-1 RNAi cells. Therefore, cells were cotransfected with $G\alpha_s$-GFP, $G\beta_1$, and $G\gamma_2$ in all imaging studies of C6 and Cav-1 RNAi cells. $G\alpha_s$-GFP expression was compared with endogenous $G\alpha_s$ expression using immunoblotting and was approximately 3-fold higher than endogenous $G\alpha_s$ expression. For the TSHR studies and cAMP generation, the cDNA encoding the human thyroid-stimulating hormone receptor was cloned into pcDNA3.1zeo by Dr. Gilbert Vassart (Institut de Recherche Interdisciplinaire, Brussels, Belgium) and generously provided by Dr. Deborah Segaloff (University of Iowa, Iowa City, IA) (Mizrachi and Segaloff, 2004). C6 cells plated in 12-well dishes were transfected with 1.0 μg of human TSHR cDNA/well using a ratio of 1:5 DNA/SuperFect transfection reagent (QIAGEN). Twenty-four later, cells were treated with bovine TSH and assayed for cAMP accumulation.

Microscopy and Live-Cell Imaging. One hour before live cell imaging, complete media was replaced with serum-free DMEM supplemented with 20 mM HEPES. Cells were maintained at 37°C during the entire period of observation using a heated microscope stage (Biotechnics; Thermo Fisher Scientific). Fluorescent images were obtained using an inverted Nikon Eclipse TE 300 microscope equipped for fluorescent microscopy as described previously (Allen et al., 2005). All images shown were obtained using oil immersion with a 60× objective. Scale bars shown are 10 μm in length. Cells were treated with 10 μM isoproterenol (Sigma, St. Louis, MO), and $G\alpha_s$-GFP trafficking was imaged in real-time during receptor stimulation. For imaging studies using the cholesterol chelating agent methyl-β-cyclodextrin (Sigma), C6 cells expressing $G\alpha_s$-GFP were preincubated with 10 mM cyclodextrin for 30 min at 37°C, and cells were washed and subsequently imaged during treatment with 10 μM isoproterenol. Images of live cells shown are representative of 40 to 50 cells imaged in six or more independent experiments. Quantification of the internalization of $G\alpha_s$-GFP was done as described previously (Yu and Rasenick, 2002; Allen et al., 2005). In brief, an individual blind to experimental conditions measured the mean gray value within the cytoplasm of cells in fluorescence images by selecting the maximal cytoplasmic region of each cell using ImageJ (http://rsbweb.nih.gov/ij/). Mean gray values of the $G\alpha_s$-GFP fluorescence in the cytoplasm were calculated and normalized to area measured.

Isolation of Lipid Rafts/Caveolae. C6 cells or Cav-1 RNAi cells were used to prepare Triton-insoluble, caveolin-enriched membrane fractions by the procedure described by Toki et al. (1999) and Allen et al. (2005), with slight modification. C6 glioma cells or Cav-1 RNAi cells were grown in 150-cm^2 flasks until confluent and incubated in serum-free DMEM for 1 h before all treatments. Two flasks of cells were harvested into 1.0 ml of ice-cold HEPES buffer (10 mM HEPES, pH 7.5, 150 mM NaCl, 1 mM DTT, and 0.3 mM phenylmethylsulfonyl fluoride) containing protease inhibitors (Complete; Roche Diagnostics, Indianapolis, IN). Cells were homogenized with 10 strokes of a motorized Potter-Elvehjem homogenizer, nuclei were removed by centrifugation at 1000*g* for 10 min, and total cellular membranes were obtained from the supernatant by 100,000*g* ultracentrifugation. The total membrane pellet was resuspended into HEPES buffer containing 1% Triton X-100 and incubated on ice for 30 min. The homogenate was adjusted to 40% sucrose by addition of an equal volume of 80% sucrose prepared in HEPES buffer, and placed at the bottom of an ultracentrifuge tube. A step gradient containing 30, 15, and 5% sucrose was formed above the homogenate and centrifuged at 200,000*g* in a SW55 rotor for 18 h. Two or three opaque bands containing the Triton X-100 insoluble floating rafts/caveolae were confined between the 15 and 30% sucrose layers. Ten 0.5-ml fractions were removed from the top of the sucrose gradients and immediately frozen in liquid nitrogen. To obtain samples of the buoyant fractions (BF) enriched in caveolae/lipid rafts, fractions 3, 4, and 5 were obtained and combined, diluted 3-fold with HEPES buffer, and pelleted in a microcentrifuge at 16,000*g* to obtain pellets of caveolin enriched samples of lipid rafts/caveolae. To obtain samples of the nonbuoyant, Triton X-100-soluble membranes or heavy fractions (HF), 200 μl was removed from the bottom of each ultracentrifuge tube (fraction 10) in the 40% sucrose layer. These HF protein samples were precipitated with 1 mM trichloroacetic acid in HEPES buffer for 30 min on ice, followed by pelleting in a microcentrifuge and resuspension in HEPES buffer after brief sonication. These samples of HF Triton X-100 soluble membranes and BF Triton X-100 insoluble lipid rafts/caveolae were subsequently analyzed for protein content by immunoblotting.

Immunoblotting. In experiments assessing total levels of proteins, C6 cells or Cav-1 RNAi cells were placed in lysis buffer (PBS/0.1% SDS) followed by brief sonication and equal protein (20 μg) of lysates were subjected to SDS-PAGE. In studies assessing protein content in isolated lipid rafts/caveolae, all 10 fractions obtained from sucrose gradients were examined by loading equal volumes of each fraction (30 μl) into 12% polyacrylamide gels followed by SDS-PAGE. In studies comparing lipid raft/caveolae buoyant fractions and heavy fractions, equal protein (5 μg) of the Triton X-100 soluble membrane fraction (fraction 10) or lipid raft/caveolae fractions (pooled fractions 3, 4, and 5) were subjected to SDS-PAGE. After electrophoresis, proteins were transferred to polyvinylidene difluoride membranes that were analyzed by Western blotting as described previously (Allen et al., 2005). After blocking and thorough washing, membranes were incubated with polyclonal rabbit $G\alpha_s$ antibody (1:10,000 dilution, 3 h; PerkinElmer Life and Analytical Sciences, Waltham, MA) or polyclonal rabbit $G\alpha_s$ antibody with overnight incubation (1:1000 dilution; Calbiochem, San Diego, CA), a polyclonal β_2AR antibody with overnight incubation (1:200 dilution; Santa Cruz Biotechnology), polyclonal AC VI antibody with overnight incubation (1:500 dilution; Santa Cruz Biotechnology), or monoclonal anti caveolin-1 antibody with 2 h incubation (1:5000 dilution; Transduction Laboratories). Detection of bound antibody on the blot was assessed using horseradish peroxidase-conjugated secondary antibodies (Jackson ImmunoResearch Laboratories Inc., West Grove, PA), visualized by enhanced chemiluminescence detection (Amersham, Chalfont St. Giles, Buckinghamshire, UK), and quantified after scanning densitometry using ImageQuant software (GE Healthcare, Chalfont St. Giles, Buckinghamshire, UK). Immunodetected $G\alpha_s$, β_2AR, AC VI, and caveolin-1 bands were quantified, and the integrated optical density of each band was determined and expressed as a percentage of wild-type C6 cells. For several of the experiments, the original membranes were stripped with an acidic glycine buffer for 5 min at room temp (100 mM glycine, pH 2.4), washed, and reprobed sequentially using the antibodies.

cAMP Accumulation Assays.

tk;2The cAMP accumulation assay was done according to the method of Salomon (1979) with slight modification. To measure cAMP accumulation in living cells, subconfluent C6 cells or Cav-1 RNAi cells were incubated for 20 h with 4 μCi/ml [2,8-^{3}H]adenine in complete media to label the total pool of cellular ATP. Before treatments, cells were washed and incubated in serum-free DMEM (containing 40 mM HEPES, 40 mM Tris, and 1 mM EGTA at pH 7.40), and pretreated with 500 μM 3-isobutyl-1-methylxanthine (IBMX), a broad species phosphodiesterase inhibitor, for 5 min to prevent cAMP degradation. Cells were subsequently exposed to agonist or drug at 37°C for 30 min at the following concentrations: 10 pM to 10 μM isoproterenol (Sigma), 0.01 to 100 mIU/ml bovine TSH (Sigma), and 100 μM forskolin (Alomone Labs, Jerusalem, Israel). In some assays, cells were pretreated as follows: 10 mM methyl-β-cyclodextrin (Sigma) for 30 min followed by agonist treatments, pretreated for 90 min with cyclodextrin-cholesterol complexes (10–1000 μg/ml cholesterol-cyclodextrin in a molar ratio of 1:6; Sigma) followed by agonist pretreatment for 18 h with 10 to 100 ng/ml pertussis toxin (Sigma) followed by agonist. Reactions were stopped and cells lysed by addition of ice-cold 5% trichloroacetic acid. Cell lysates were incubated on ice for 1 h, and cell debris was removed by centrifugation. [α-^{32}P]ATP and [8-^{14}C]cAMP (1000 cpm each) were added as internal standards to each sample. [2,8-^{3}H]ATP and [2,8-^{3}H]cAMP were separated by sequential Dowex-Alumina ion exchange column chromatography and eluates collected into vials followed by scintillation counting for ^{3}H, ^{32}P, and ^{14}C. Normalizing to [2,8-^{3}H]ATP served to control for variations in cell number and metabolism un-

related to adenylyl cyclase activity. Variations in column recovery were corrected for using the [8-^{14}C]cAMP counts. Data were expressed as cAMP formed/(ATP formed + cAMP formed) × 100%.

Adenylyl Cyclase Activity Assays. Adenylyl cyclase enzyme activity assays in cell membranes were also performed according to the method of Salomon (1979), with slight modification. Initially, C6 cell membranes from cells were obtained by centrifugation as follows. A confluent 150-cm^2 flask of cells was harvested, cells resuspended in 1 ml of ice-cold HEPES/sucrose buffer [10 mM HEPES, 1 mM DTT, 0.25 M sucrose, and 1× protease inhibitor cocktail (Complete, Roche Diagnostics), pH 7.5] and homogenized with 10 strokes of a motorized Potter-Elvehjem homogenizer. The homogenate was centrifuged at 600*g* for 10 min, supernatant reserved, pellet resuspended again in 1 ml of ice-cold HEPES/sucrose buffer. The homogenate was centrifuged again at 1040*g* for 10 min, and a supernatant was obtained and combined with the reserved supernatant. Supernatants were ultracentrifuged at 100,000*g* for 30 min, and membrane pellets obtained and resuspended in 700 μl of HEPES buffer (15 mM HEPES buffer, 1× protease inhibitor cocktail, pH 7.5). Samples were stored under liquid N_2 until use. Ten micrograms of cell membranes were added to a reaction mixture containing agonists or drugs for 20 min at 30°C to allow the conversion of [α-^{32}P]ATP to [α-^{32}P]cAMP in a buffer containing IBMX and an NTP-regeneration system (2.5 μCi/ml [α-^{32}P]ATP, 15 mM HEPES, 5 mM $MgCl_2$, 1 mM EGTA, 1 mM DTT, 500 μM IBMX, 10 μM GTP, 0.25 mg/ml bovine serum albumin, 50 μM cAMP, 50 μM ATP, 0.14 mg/ml creatine phosphokinase, and 0.5 mg/ml creatine phosphate). The reaction was stopped on ice with 1% SDS, 45 mM ATP, and 1.3 mM cAMP, and 10,000 cpm of [2,8-^{3}H]cAMP was added as an internal standard to adjust for recovery. cAMP was purified using sequential Dowex-Alumina column chromatography, eluates collected followed by scintillation counting for ^{3}H and ^{32}P. Adenylyl cyclase activity was expressed as picomoles of cAMP formed per minute per milligram of protein after normalizing for column recoveries (Salomon, 1979). A standard curve analysis determined that 10 μg of membrane protein used in these assays was within the linear range of adenylyl cyclase enzyme activity.

Cholesterol Measurements. Total cell lysates or membranes from wild-type C6 or Cav-1 RNAi cells were prepared as follows. For total lysates, confluent cells grown in 75-cm^2 flasks were harvested into ice-cold PBS, pelleted by brief centrifugation, and resuspended in 1 ml of HEPES buffer (15 mM HEPES, 1 mM DTT, and 1× protease inhibitor cocktail, pH 7.5). Total lysates were obtained by homogenizing the cells with 10 strokes of a motorized Potter-Elvehjem homogenizer. Membranes were prepared as described for adenylyl cyclase activity assays. Whole-cell lysates and crude membrane pellets were submitted to the Pathology Department at UIC for cholesterol analysis. Samples were analyzed on the SYNCHRON CX System using a cholesterol reagent kit in conjunction with the SYNCHRON Systems CX MULTI Calibrator (Beckman Coulter, Fullerton, CA). The reaction uses cholesterol oxidase and the hydrolysis of cholesterol esters into free cholesterol and the oxidation of free cholesterol, producing hydrogen peroxide. The result is quantified by a peroxidase-generated color reaction and analyzed by automated spectrophotometry. Results obtained in micrograms of cholesterol per deciliter were normalized to protein concentration in the samples and are expressed as micrograms of cholesterol per milligram of protein.

Statistical Analyses. All quantified data were analyzed for statistical significance using a one-way ANOVA followed by Student-Newman-Keuls multiple comparison test using Prism 4.0 software (GraphPad Software Inc., San Diego, CA). Differences were considered significant at $p < 0.05$. E_{max} and EC_{50} values of agonist responses were calculated by nonlinear regression sigmoidal best-fit curve analysis using Prism 4.0.

Results

Stable Knockdown of Caveolin-1 in C6 Glioma Cells as a Model System. As a simplified cell system, we used C6 glioma cells in which caveolin-1 is stably knocked-down by RNA interference. Because caveolin knockdown might influence the overall expression of βAR signaling molecules, total protein levels were examined in Cav-1 RNAi cells and compared with WT C6 cells. It is worth noting that stable knockdown of caveolin-1 in these cells also results in knockdown of caveolin-2 (Bhatnagar et al., 2004). Total protein lysates from both cell types were obtained and equal protein subjected to SDS-PAGE followed by immunoblotting (Fig. 1A). Cav-1 RNAi cells showed significantly reduced immunoreac-

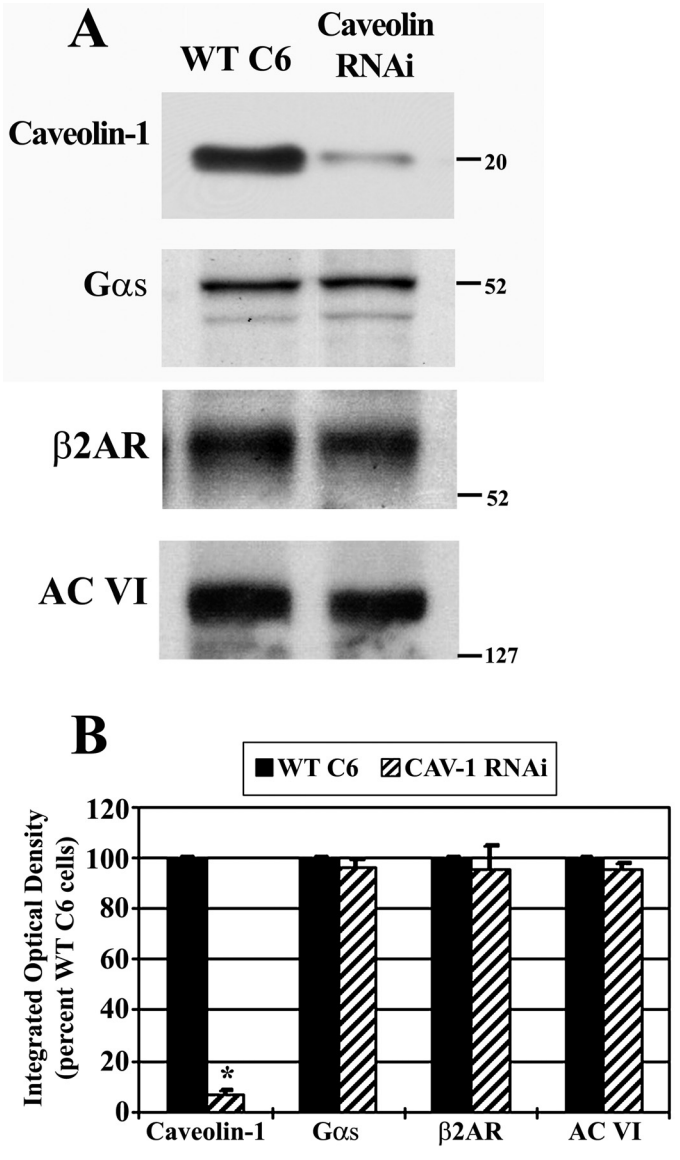

Fig. 1. Stable knockdown of caveolin-1 has no effect on the content of β-adrenergic-related signaling molecules. Total protein lysates from wild-type C6 or stable caveolin-1 knockdown cells were analyzed by SDS/PAGE and immunoblotting to determine relative protein levels of caveolin-1, $G\alpha_s$, β_2AR, and AC type VI. A, immunoreactivity from a representative immunoblot is shown, where the blot was stripped and reprobed sequentially for each protein. B, blots were quantified by scanning densitometry, and data were pooled from four independent experiments and are expressed as a percentage of wild-type C6 cells ($n = 4$). *, $p < 0.05$ versus WT C6.

tivity for caveolin-1 (reduced by ~90% versus WT C6 cells). Blots were stripped and sequentially reprobed for total levels of β_2AR, $G\alpha_s$, and adenylyl cyclase type 6 (AC VI), the predominant AC isoform in C6 cells (Debernardi et al., 1993). Although a slight decrease in the levels of proteins is evident in the representative immunoblot (Fig. 1A), the mean integrated optical density obtained from scanning densitometry of blots from four independent experiments showed no change in total protein levels of β_2AR, $G\alpha_s$, or AC VI in the Cav-1 RNAi cells versus WT C6 cells (Fig. 1B). These results confirm stable knockdown of caveolin-1 protein in Cav-1 RNAi cells and reveal no major alteration in the level of signaling molecules in the βAR-$G\alpha_s$-adenylyl cyclase signaling cascade.

Caveolin Knockdown Decreases $G\alpha_s$ Localization and Adenylyl Cyclase Activity in Lipid Rafts/Caveolae. Although the total level of $G\alpha_s$ seemed unchanged by caveolin RNAi, the membrane distribution of $G\alpha_s$ might be altered by this genetic disruption. To examine the distribution of endogenous $G\alpha_s$ in lipid rafts/caveolae, WT C6 and Cav-1 RNAi cell membranes were isolated and subjected to solubilization in 1% Triton X-100. Detergent resistant raft/caveolae enriched membranes were then isolated by sucrose density gradient fractionation (Fig. 2). Ten membrane fractions from each cell type were isolated and equal volumes from each fraction analyzed by immunoblotting for endogenous $G\alpha_s$ or caveolin-1 (Fig. 2, A and B). Results from WT C6 cells indicated that caveolin-1 containing fractions were exclusively located in buoyant sucrose fractions 3, 4, and 5 (Fig. 2A, bottom). In Cav-1 RNAi cells, caveolin-1 immunoreactivity was greatly decreased and detected in only buoyant fraction 5 (Fig. 2B, bottom). In the unstimulated WT C6 cells, $G\alpha_s$ immunoreactivity was located predominantly in the heavy sucrose fractions containing detergent soluble membranes; however, approximately 15 percent of $G\alpha_s$ immunoreactivity was located in the caveolin-containing fractions (Fig. 2A, top). In the Cav-1 RNAi cells, $G\alpha_s$ immunoreactivity was shifted and decreased in fractions 3, 4, and 5 compared with WT C6 cells (Fig. 2B, top).

To further examine this raft/caveolae distribution of $G\alpha_s$, fractions 3, 4, and 5 were combined and represent the TX-100 insoluble BFs enriched in rafts/caveolae, and a heavy sucrose fraction (fraction 10) was isolated and is representative of the nonraft membranes. This analysis enables a relative comparison of $G\alpha_s$ content in raft/caveolae versus nonraft/caveolae fractions between the two conditions but does not represent the total $G\alpha_s$ membrane content. Equal protein (5 μg) of BF and HF were analyzed by immunoblotting (Fig. 2C). This equal protein comparison showed that $G\alpha_s$ immunoreactivity was enriched in BF lipid rafts/caveolae compared with the nonraft HF. It is noteworthy that the localization of $G\alpha_s$ in BF was decreased in Cav-1 RNAi cell membranes compared with WT C6 membranes (Fig. 2C, top). Quantification of $G\alpha_s$ bands by scanning densitometry determined that $G\alpha_s$ localized in BF rafts/caveolae was significantly decreased by ~50% in Cav-1 RNAi cells versus WT C6 cells (Fig. 2D). These data indicate stable knockdown of caveolin-1 decreases $G\alpha_s$ localization in lipid rafts/caveolae, suggesting that caveolin-containing microdomains localize a portion of $G\alpha_s$ to buoyant membrane fractions. These findings are consistent with the previous finding that $G\alpha_s$ is located in detergent resistant membrane fractions of C6 cells and that β-agonist stimulation increases the pool of G protein located in these membrane domains (Allen et al., 2005).

In a complementary experiment, AC enzyme activity in the membrane fractions was determined. The picomoles of cAMP generated from each fraction were expressed as a percentage of total response from all fractions. This normalization enabled comparison of the relative AC activity present in each fraction (Fig. 2E). This analysis showed the majority of total cAMP synthesis (~70%) occurred in non–raft-containing heavy fractions 8, 9, and 10 in both WT C6 and Cav-1 RNAi cells. It is noteworthy that Cav-1 RNAi cells showed a reduction in cAMP synthesis in buoyant fractions 3, 4, and 5, suggesting that caveolin knockdown redistributes adenylyl cyclase from lipid rafts/caveolae to nonraft membrane regions.

Disruption of Lipid Rafts/Caveolae with Cyclodextrin or Caveolin Knockdown Increases βAR and TSHR-Stimulated cAMP Accumulation. To examine the effects of disrupting lipid rafts/caveolae on βAR signaling, WT C6 cells were treated with methyl-β-cyclodextrin (a cholesterol chelating agent that disrupts these membrane domains) and isoproterenol-stimulated cAMP accumulation was determined (Fig. 3A). Pretreatment of cells with cyclodextrin increased isoproterenol-stimulated cAMP accumulation by ~60%. This increase was reversed if cholesterol was restored to the cyclodextrin-treated cells. Cyclodextrin had no detectable effect on basal cAMP levels.

Agonist-stimulated cAMP accumulation studies were also performed with Cav-1 RNAi cells (Fig. 3B). Both WT and Cav-1 RNAi cell lines were treated with increasing concentrations of isoproterenol (10 pM–1 μM) for 30 min basal cAMP levels were unchanged in caveolin knockdown cells when data from six independent experiments were combined (basal cAMP means ± S.E.: WT C6, 0.24 ± 0.36; Cav-1 RNAi, 0.43 ± 0.16). Data were processed by nonlinear regression best-fit curve analysis to obtain agonist potencies (EC_{50}) and efficacies (E_{max}). Isoproterenol-stimulated cAMP accumulation was increased approximately 80% in Cav-1 RNAi cells versus WT C6 cells (E_{max} values: WT C6,14.66 ± 0.29; Cav-1 RNAi, 23.33 ± 0.23). However, agonist potency was unchanged by caveolin-1 knockdown (EC_{50} values: WT C6, 6.54 nM; Cav-1 RNAi, 5.13 nM; EC_{50} 95% confidence intervals: WT C6, 5.14–8.33 nM; Cav-1 RNAi, 4.36–6.05 nM). These data suggest that stable knockdown of caveolin increases maximal isoproterenol-stimulated cAMP accumulation without altering agonist potency.

To determine whether signaling from another $G\alpha_s$-coupled GPCR is similarly affected by caveolin knockdown, WT C6 and Cav-1 RNAi cells were treated with bovine TSH, because gene array studies of C6 cells have reported detection of TSHR mRNA (Bhatnagar et al., 2004). Treatment of cells with saturating concentrations of TSH did not result in increased cAMP production, indicating that endogenous TSH receptors are not functional or that TSHR protein is not expressed in C6 cells (data not shown). As an alternative approach, cells were transfected with a human TSHR construct and 24 h after transfection treated with increasing concentrations of TSH (0.01 to 100 mIU/ml). TSH-stimulated cAMP accumulation was significantly increased in Cav-1 RNAi cells versus WT C6 cells at all concentrations of TSH tested (Fig. 3C), suggesting that both βAR and TSHR signaling is increased by caveolin knockdown. Taken together,

these data indicate that disrupting lipid rafts/caveolae in C6 cells greatly increases βAR or TSHR signaling, suggesting that these membrane microdomains attenuate $G\alpha_s$-coupled GPCR signaling.

Caveolin Knockdown Increases Forskolin- and Fluoride-Stimulated $G\alpha_s$/Adenylyl Cyclase Signaling. To clarify whether signaling elements downstream of the receptor are responsible for the elevated cAMP observed in the Cav-1 RNAi cells, cells were treated with isoproterenol, forskolin, or fluoride, and cAMP accumulation was determined. Forskolin binds directly to adenylyl cyclase and is capable of activating the enzyme. Nonetheless, AC activation by forskolin is also strongly influenced by the presence and activation of $G\alpha_s$ (Sutkowski et al., 1994; Insel and Ostrom, 2003). Forskolin binding affinity at AC is highest when $G\alpha_s$ is present, and labeled forskolin can be used to detect and characterize $G\alpha_s$-AC complexes in cells and membranes as well as assess basal $G\alpha_s$ activation of AC (Insel and Ostrom, 2003). Experiments testing forskolin determined isoproterenol as well as forskolin-stimulated cAMP accumulation was significantly increased in Cav-1 RNAi cells compared with WT C6 cells (Fig. 4A).

To further confirm that caveolin knockdown potentiated $G\alpha_s$-AC signaling, adenylyl cyclase enzyme activity assays were performed in membrane preparations isolated from WT C6 or Cav-1 RNAi cells. Results revealed basal adenylyl cyclase activity was similar in membrane preparations from WT C6 cells and Cav-1 RNAi cells (Fig. 4B; unstimulated cells: WT C6 = 13.74 ± 0.81 pmol of cAMP/min/mg; Cav-1 RNAi = 16.84 ± 1.56 pmol of cAMP/min/mg). Forskolin-

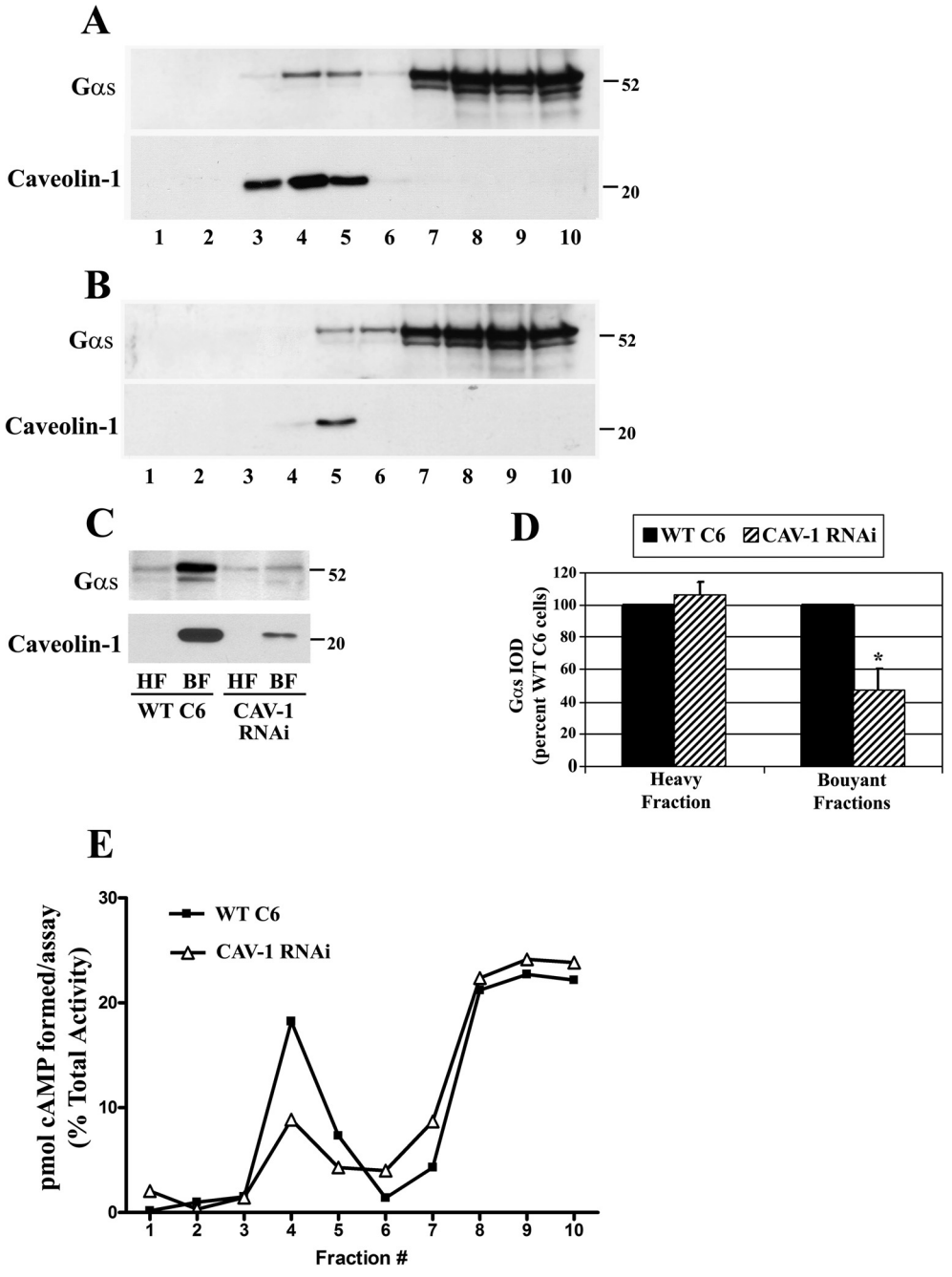

Fig. 2. Caveolin knockdown decreases $G\alpha_s$ localization and adenylyl cyclase activity in lipid rafts/caveolae. Membranes from wild-type C6 or stable caveolin-1 knockdown cells (Cav-1 RNAi) were homogenized, incubated with 1% Triton X-100 followed by sucrose density gradient fractionation and immunoblotting for endogenous $G\alpha_s$ or caveloin-1. A, representative immunoblot of $G\alpha_s$ (top) or the same blot reprobed for caveoin-1 (bottom) in the 10 fractions isolated from wild-type C6 cells where equal volumes were loaded from each fraction. B, representative immunoblots of $G\alpha_s$ (top) or caveolin-1 (bottom) in fractions obtained from stable caveolin knockdown cells where equal volumes were loaded from each fraction. C, buoyant sucrose fractions 3, 4, and 5 enriched in caveolin (BF), as well as the heavy sucrose fraction number 10 (HF) were isolated, and equal protein concentrations from the fractions were loaded and analyzed by immunoblotting for $G\alpha_s$ (top) or caveolin-1 (bottom). D, quantification of $G\alpha_s$ immunoreactivity in the sucrose heavy fraction or buoyant fractions. Blots were quantified by scanning densitometry, and data were pooled from three independent experiments and are expressed as a percentage of wild-type C6 cells ($n = 3$). *, $p < 0.05$ versus wild-type C6 cells. E, 50 μl of each isolated fraction was incubated in an adenylyl cyclase reaction mix containing 50 μM forskolin and ^{32}P-ATP. [^{32}P]cAMP was isolated and total picomoles of cAMP formed in each fraction was determined through scintillation counting. These values were converted to a percentage of total aggregate activity of adenylyl cyclase present in each isolated fraction. Data presented are representative of similar results from two independent experiments.

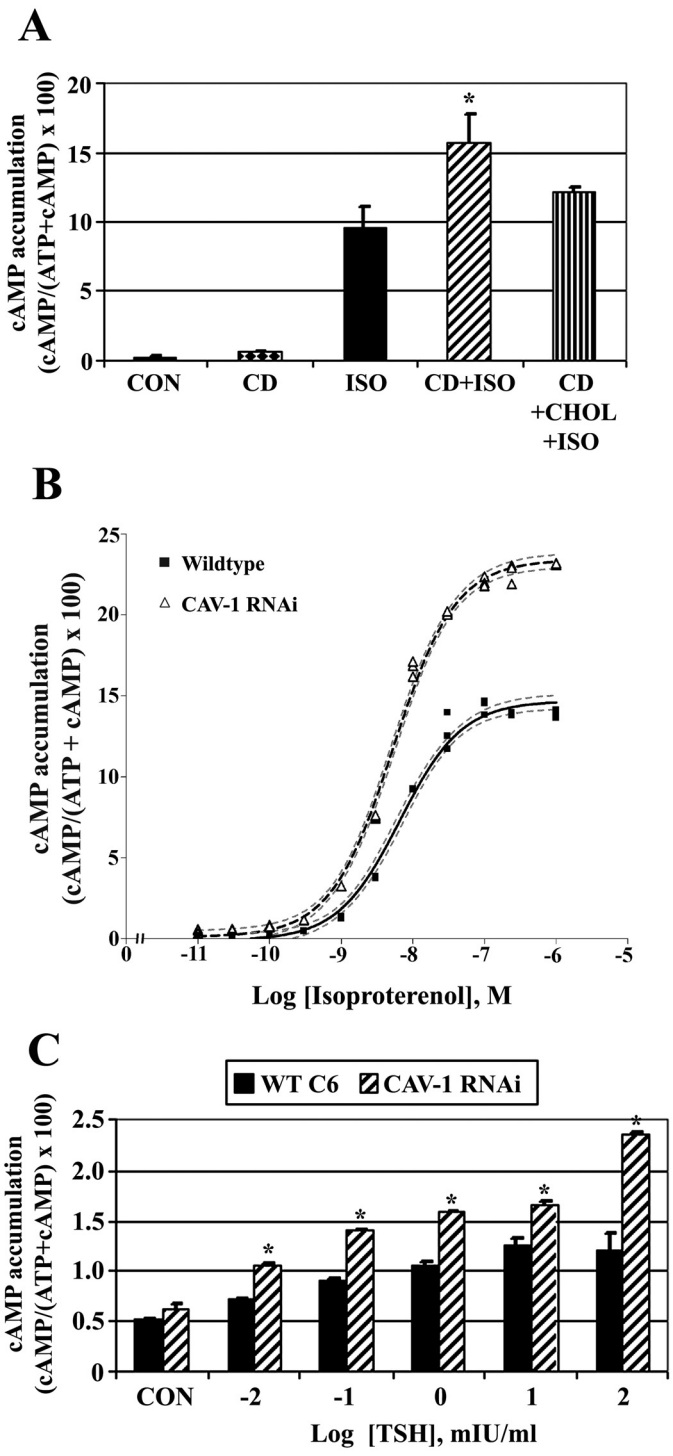

Fig. 3. Disruption of lipid rafts/caveolae with cyclodextrin or caveolin knockdown increases βAR and TSHR-stimulated cAMP accumulation. Wild-type C6 cells were incubated with [2,8-^{3}H]adenine for 18 h to label cellular ATP. A, cells were treated initially with ± 10 mM methyl-β-cyclodextrin (CD) for 30 min to disrupt lipid rafts/caveolae, or with CD followed by CD-cholesterol complexes (CD+CHOL) for 90 min to restore cholesterol to the cells. Intact cells were subsequently treated with 10 μM isoproterenol (ISO) for 30 min and [2,8-^{3}H]cAMP accumulation was determined. Data presented are the means ± S.E.M. from six independent experiments performed in triplicate ($n = 6$). *, $p < 0.05$ versus ISO-treated cells. B, wild-type C6 cells or caveolin-1-stable knockdown cells (CAV-1 RNAi) were incubated with [2,8-^{3}H]adenine for 18 h to label cellular ATP. Intact cells were treated with increasing concentrations of ISO for 30 min and [2,8-^{3}H]cAMP accumulation was determined. Data are the means ± S.E.M. from a single dose-response experiment performed in triplicate with similar results observed in three independent experiments. C, wild-type C6 cells or CAV-1 RNAi cells were transiently transfected with human thyrotropin (TSH) receptor and 24 h later were incubated with [2,8-^{3}H]adenine for 18 h to radioactively label cellular ATP. Intact cells were treated with increasing concentrations of TSH for 30 min, and [2,8-^{3}H]cAMP accumulation was determined. Data are the means ± S.E.M. from three independent experiments. *, $p < 0.05$ versus WT C6 cells for each treatment group.

stimulated adenylyl cyclase activity was increased by ~80% in membranes from Cav-1 RNAi cells versus WT C6 cells (Fig. 4B).

Aluminum tetrafluoride (AlF_4^-) was used to directly activate $G\alpha_s$ to assess $G\alpha_s$-stimulated adenylyl cyclase activity. Fluoride stimulation of adenylyl cyclase is routinely attributed to AlF_4^- mimicking the terminal phosphate of GTP, thus activating the GDP form of $G\alpha_s$ in a hormone-independent fashion. Fluoride-stimulated AC activity was increased by 112% in Cav-1 RNAi versus WT C6 membranes, indicating that stable caveolin knockdown increases $G\alpha_s$-stimulated activation of AC (Fig. 4C). Taken together, these data suggest that stable knockdown of caveolin enhances cAMP accumulation and AC activity downstream of the βAR at the level of $G\alpha_s$/AC. These results also imply that $G\alpha_s$/AC signaling is attenuated by the presence of caveolins/caveolae.

Increased Camp Accumulation Due to Caveolin Knockdown Is Cholesterol and $G\alpha_i$ Independent. Caveolin binds tightly to cholesterol (Murata et al., 1995) and has been implicated in regulating intracellular cholesterol transport (Smart et al., 1996) as well as regulating cholesterol homeostasis in cells and tissues (Frank et al., 2006). This intimate association between caveolin and cholesterol raises the possibility that alterations in cholesterol may occur due to the stable knockdown of caveolin. Because membrane fluidity and several membrane-associated proteins are influenced by cholesterol content, the increased cAMP effects observed with Cav-1 RNAi cells might be due to in part altered cholesterol. To test this, WT C6 and Cav-1 RNAi total cell lysates or membranes were prepared and analyzed for cholesterol content. As a positive control, WT C6 cells were treated with cyclodextrin to chelate cholesterol, using the same treatment paradigm as done in previous experiments. Cholesterol content in total lysates or membranes was similar in WT C6 and Cav-1 RNAi cells; however, cyclodextrin treatments decreased total and membrane cholesterol (Fig. 5A).

After this, WT C6 and Cav-1 RNAi cells were dose-treated with exogenous cholesterol, followed by measurements of cAMP accumulation (Fig. 5B). In the absence of agonist, cholesterol treatments had no effect on basal cAMP in either cell type. The highest concentration of cholesterol tested (1 mg/ml) significantly attenuated isoproterenol-stimulated cAMP accumulation in both WT C6 and Cav-1 RNAi cells. These results and the observation that cholesterol content was unchanged by caveolin knockdown, suggest that the signaling effects observed in the Cav-1 RNAi cells are independent of cholesterol content.

Upon phosphorylation by PKA, β_2ARs can switch coupling to $G\alpha_i$, an event shown to be involved in $G\beta\gamma$ mediated-activation of MAPK signaling cascades and ERK1/2 activation (Daaka et al., 1997). In addition, caveolae have been implicated in regulating the physiologic signaling of β_2AR subtypes in cardiomyocytes and may influence the coupling of $G\alpha_i$ (Rybin et al., 2000; Xiang et al., 2002). This $G\alpha_i$

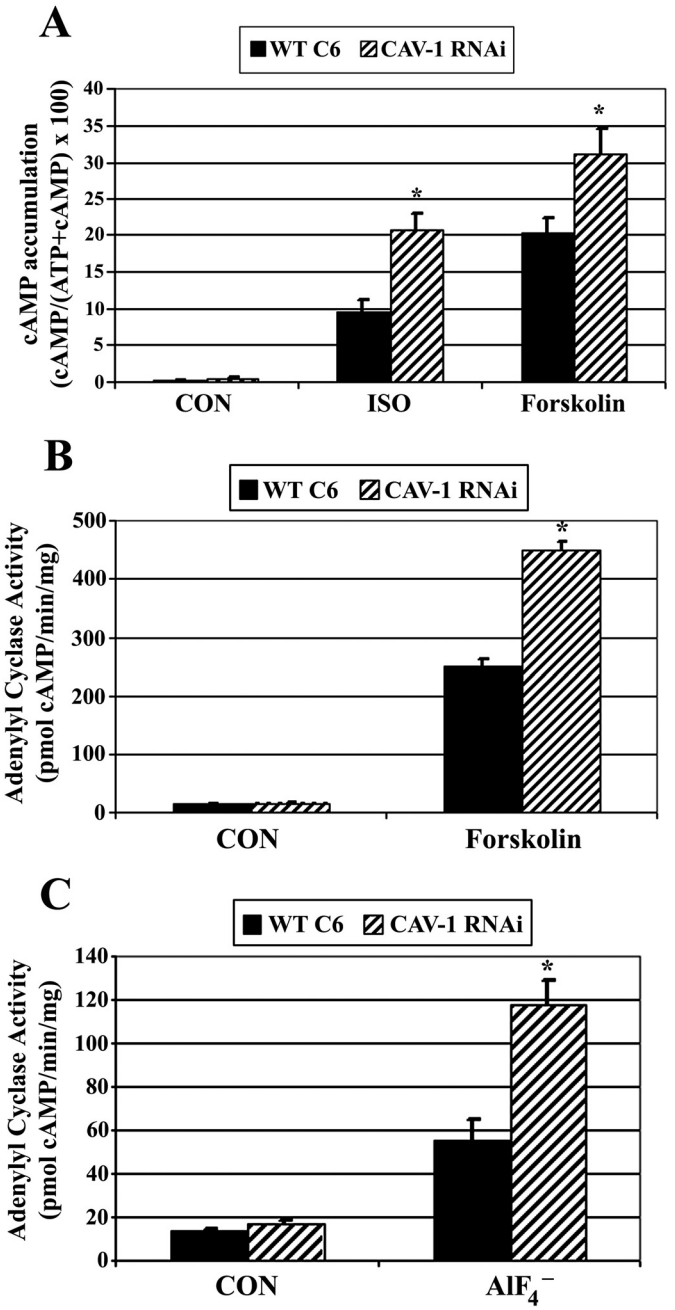

Fig. 4. Caveolin knockdown increases forskolin- and fluoride-stimulated $G\alpha_s$/adenylyl cyclase signaling. A, wild-type C6 cells (WT C6) or caveolin-1 stable knockdown cells (CAV-1 RNAi) were incubated with [2,8-^{3}H]adenine for 18 h to label cellular ATP. Intact cells were treated with ± 10 μM isoproterenol (ISO) or 100 μM forskolin for 30 min, and [2,8-^{3}H]cAMP accumulation was determined. Data presented are the means ± S.E.M. from six independent experiments performed in triplicate ($n = 6$). *, $p < 0.05$ versus WT C6 cells for each treatment group. B, adenylyl cyclase activity was determined in cell membranes isolated from WT C6 or CAV-1 RNAi cells. Membranes were incubated with ± 50 μM forskolin for 20 min [^{32}P]cAMP was isolated and determined by scintillation counting, normalized to time and milligrams of membrane protein. Data presented are the means ± S.E.M. from a single experiment performed in triplicate and are representative of similar results observed in three independent experiments. C, adenylyl cyclase activity was determined in cell membranes isolated from WT C6 or CAV-1 RNAi cells. Membranes were incubated for 20 min with a reaction mixture including ^{32}P-ATP and ± 10 mM sodium fluoride/20 μM aluminum chloride. [^{32}P]cAMP was isolated and determined by scintillation counting, normalized to time and milligrams of membrane protein. Data presented are the means ± S.E.M. from an experiment performed in triplicate and is representative of similar results observed in four independent experiments.

switching mechanism might be influenced by lipid rafts/caveolae, potentiating adenylyl cyclase by diminished inhibition. To test this, $G\alpha_i$/$G\alpha_o$ subunits were prevented from coupling to β_2ARs by treating cells with pertussis toxin (PTX). PTX treatments did not alter basal or isoproterenol-stimulated cAMP accumulation in WT C6 or Cav-1 cells (Fig. 5C), and the elevated cAMP production in Cav-1 RNAi cells was unaffected by inactivating $G\alpha_i$ coupling to the β_2AR. The lack of effect of PTX on isoproterenol-stimulated cAMP in WT C6 cells is consistent with previous findings (Watts and Neve, 1996). PTX uncouples receptors from $G\alpha_i$/$G\alpha o$; however, it does not inactivate those G proteins. Therefore, in the absence of constitutively active receptors, PTX should not increase $G\alpha_s$ activity. These results indicate the elevated $G\alpha_s$/adenylyl cyclase signaling resulting from caveolin knockdown is independent of $G\alpha_i$.

Agonist-Induced Internalization of $G\alpha_s$-GFP Requires Lipid Rafts and Caveolins. Our previous trafficking studies indicated that stimulation of βARs in C6 cells resulted in the internalization of $G\alpha_s$-GFP through lipid rafts (Allen et al., 2005). To distinguish contributions of cholesterol and/or caveolins to this trafficking, $G\alpha_s$-GFP localization was further examined using Cav-1 RNAi cells and wild-type cells. It is worth noting that $G\alpha_s$-GFP is a fully functional fluorescent fusion protein that exhibits nearly identical trafficking and cellular distribution as endogenous $G\alpha_s$ (Yu and Rasenick, 2002). Wild-type C6 cells or Cav-1 RNAi cells were transfected with $G\alpha_s$-GFP, $G\beta_1$, $G\gamma_2$, and living cells imaged during treatment with 10 μM isoproterenol (Fig. 6). $G\alpha_s$-GFP imaging experiments were done in WT C6 and Cav-1 RNAi cells and compared with results using methyl-β-cyclodextrin. Isoproterenol stimulation of WT C6 cells resulted in a partial internalization of $G\alpha_s$-GFP, similar to previous observations (Yu and Rasenick, 2002; Allen et al., 2005). In the representative WT C6 cells shown, 20 min of agonist exposure increased $G\alpha_s$-GFP fluorescence in intracellular vesicles and punctate structures and also reduced the signal located at the plasma membrane (Fig. 6, A and B). Preincubation of cells with cyclodextrin prevented agonist-induced endocytosis of $G\alpha_s$-GFP; however, this was reversed in cells treated with cyclodextrin followed by cholesterol repletion (Fig. 6, C–E). It is noteworthy that agonist treatment of Cav-1 RNAi cells showed few detectable changes in $G\alpha_s$-GFP localization, and signals remained largely at the same membrane structures over the 30 min of agonist stimulation (Fig. 6, F–H). Images of $G\alpha_s$-GFP from >50 cells for each treatment group from at least six independent experiments were quantified and normalized to untreated control cells (Fig. 6I). These results reveal that $G\alpha_s$-GFP internalization is prevented by disruption of rafts/caveolae with cyclodextrin or by caveolin knockdown, suggesting that $G\alpha_s$ requires cholesterol and caveolin-1 to undergo endocytosis during βAR signaling.

Caveolin-1 Knockout Increases G_s/Adenylyl Cyclase Signaling Activity in Mouse Brain. Finally, to determine whether caveolin influences $G\alpha_s$/AC signaling in a native system, $G\alpha_s$/AC signaling was examined ex vivo in brain membranes isolated from wild-type and caveolin-1 knockout mice. Corpus striatum membranes isolated from littermate wild-type or caveolin-1 knockout mice were assayed for AlF_4^- and forskolin-stimulated AC activity. No significant difference was evident in basal AC activity between the genotypes

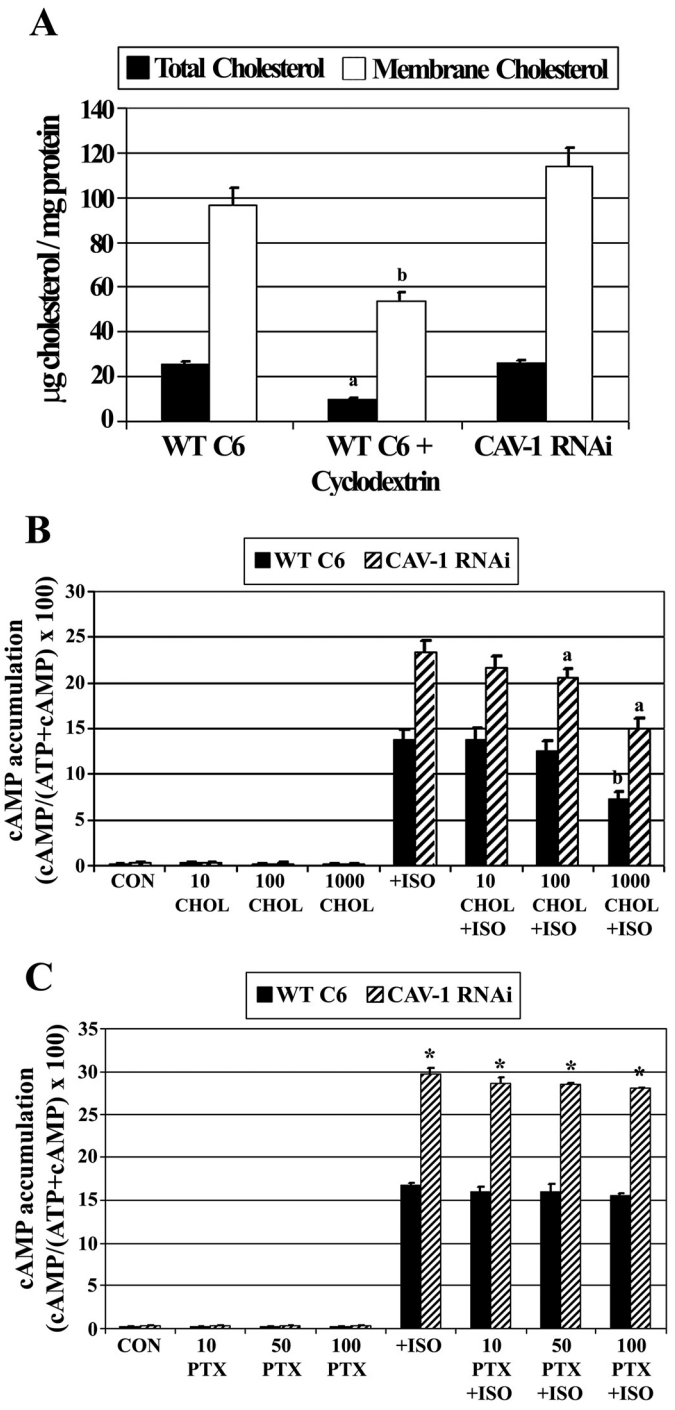

Fig. 5. Increased cAMP accumulation due to caveolin knockdown is independent of cholesterol and $G\alpha_i$. A, analysis of cholesterol content in wild-type C6 cells (WT C6) or caveolin-1 stable knockdown cells (CAV-1 RNAi). WT C6 cells were treated with ± 10 mM methyl-β-cyclodextrin for 30 min. Total cell lysates or membranes from cells were analyzed for cholesterol content. Data presented are the means ± S.E.M. from three independent experiments ($n = 3$). a, $p < 0.05$ versus total cholesterol in WT C6 cells; b, $p < 0.05$ versus membrane cholesterol in WT C6 cells. B, effects of adding exogenous cholesterol on isoproterenol-stimulated cAMP accumulation. Cells were incubated with [2,8-^{3}H]adenine for 18 h to label cellular ATP and subsequently treated with ±10, 100, or 1000 μg/ml cholesterol (CHOL) for 2 h. Intact cells were subsequently treated with ± 10 μM isoproterenol (ISO) for 30 min and [2,8-^{3}H]cAMP accumulation was determined. Data presented are the means ± S.E.M. from three independent experiments performed in triplicate. a, $p < 0.05$ versus ISO treated CAV-1 RNAi cells; b, $p < 0.05$ versus ISO-treated WT C6 cells. C, increased cAMP accumulation as a result of caveolin knockdown is independent of $G\alpha_i$ coupling. Cells were incubated with [2,8-^{3}H]adenine for 18 h to label cellular ATP. During this incubation, cells were also treated with 10, 50, or 100 ng/ml pertussis toxin (PTX), which prevents $G\alpha_i$ subunits from coupling to the βAR. Intact cells were subsequently exposed to ±10 μM ISO for 30 min and [2,8-^{3}H]cAMP accumulation was determined. Data presented are the means ± S.E.M. from three independent experiments. *, $p < 0.05$ versus WT C6 cells in each treatment group.

(Fig. 7A: WT mice basal AC activity, 13.1 ± 1.6; Cav-1 KO basal AC activity, 16.8 ± 2.3; Fig. 7B: WT mice basal AC activity, 12.0 ± 1.9, Cav-1 KO basal AC activity, 13.0 ± 1.4). However, AlF_4^--stimulated AC activity was increased by approximately 60% in caveolin-1 knockout membranes versus wild-type (Fig. 7A). In addition, forskolin-stimulated AC activity was increased approximately 30% compared with wild-type (Fig. 7B). These data suggest that genetic knockout of caveolin-1 increases $G\alpha_s$/AC signaling in mouse brain.

Discussion

The major findings of this study are that lipid rafts/caveolae and caveolin-1 exert a major effect on $G\alpha_s$ trafficking and $G\alpha_s$/AC signaling. To the best of our knowledge, this is the first investigation demonstrating genetic loss of caveolin in cells or mice results in elevated $G\alpha_s$/AC signaling. Disruption of rafts/caveolae by either genetic or pharmacological approaches prevented $G\alpha_s$ trafficking in these membrane domains, prevented $G\alpha_s$ internalization, and greatly elevated $G\alpha_s$/AC signaling. These findings support the concept that caveolins and rafts/caveolae attenuate cAMP signaling by modulating both $G\alpha_s$ trafficking and $G\alpha_s$-AC coupling. Therefore, caveolins and intact raft/caveolae microdomains might globally dampen cAMP signaling during activation of $G\alpha_s$-coupled GPCRs. Furthermore, these studies provide novel evidence to support a role for G protein mechanisms and membrane microdomains in signaling attenuation.

Lipid rafts and caveolae are typically thought of as membrane microdomains that spatially organize GPCR signaling molecules to promote kinetically favorable interactions to facilitate transduction (Ostrom and Insel, 2004). However, a survey of previous studies indicates that rafts/caveolae are equally likely to either enhance or inhibit signaling at the level of GPCR, G protein, or effector (Allen et al., 2007). Given this complexity, we used the simplified system of C6 cells to examine the effects of rafts/caveolae on GPCR/$G\alpha_s$/AC signaling. Overall, the findings indicate that caveolins and lipid rafts/caveolae attenuate cAMP signaling at the level of $G\alpha_s$/AC. In C6 cells, caveolin knockdown increased cAMP responses induced by multiple $G\alpha_s$ agonists, including isoproterenol, TSH, and AlF_4^-. In addition, experiments using fluoride or forskolin indicate that caveolin knockdown profoundly increases G_s-stimulated AC activity and cAMP accumulation without altering basal activity or cAMP levels. Because AlF_4^--stimulated or forskolin-stimulated AC activity was increased by caveolin knockdown (by 112 and 80%, respectively), these results have determined the mechanism of caveolin-1 inhibition is at the level of $G\alpha_s$/AC and distal to GPCRs.

The finding that lipid rafts/caveolae attenuate cAMP production in this report is also consistent with previous studies. A recent report from Pontier et al. (2008) similarly demonstrated that cholesterol chelation with cyclodextrin enhances

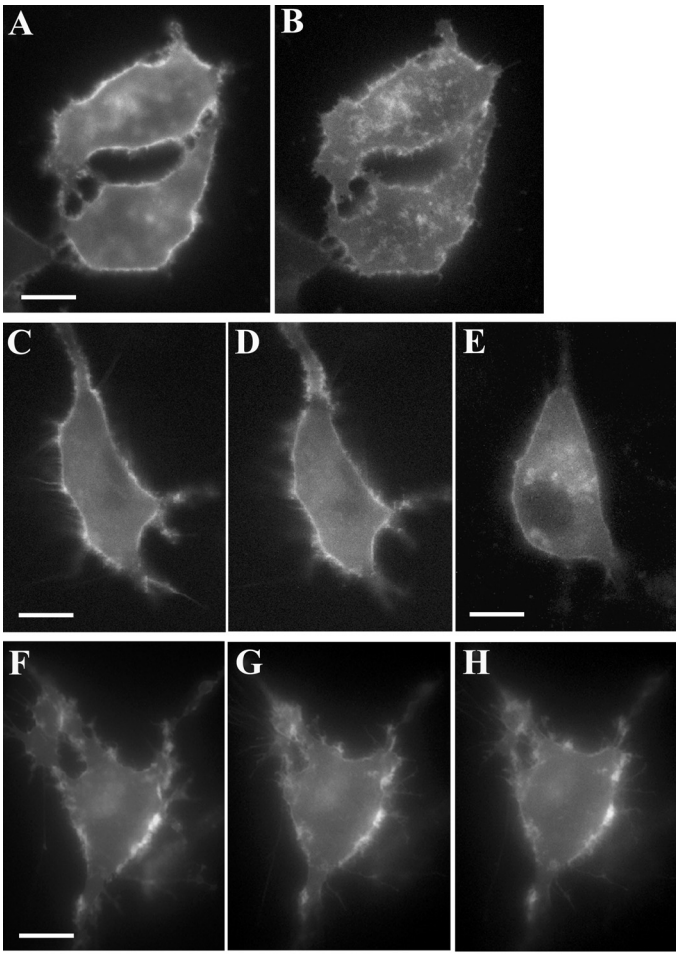

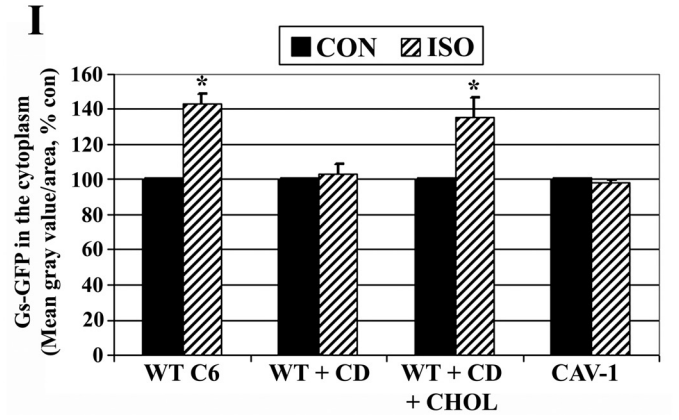

Fig. 6. Agonist-induced $G\alpha_s$ internalization requires lipid microdomains and caveolin-1. C6 glioma cells were transiently transfected with $G\alpha_s$-GFP, and trafficking was assessed using digital fluorescence microscopy. Living cells were imaged in real time, and individual frames are shown before and after 10 μM isoproterenol (ISO) treatment. A and B, $G\alpha_s$-GFP localization in wild-type C6 cells before agonist treatment (A) or after 20 min of isoproterenol stimulation (B). C to E, wild-type C6 cells expressing $G\alpha_s$-GFP were preincubated with 10 mM methyl-β-cyclodextrin (CD) for 30 min and imaged (C), and cells were subsequently treated with isoproterenol for 30 min (D). These cells were washed and incubated for 90 min with cyclodextrin-cholesterol complexes (CHOL) to restore cellular cholesterol and then were treated again with isoproterenol for 30 min (E). F to H, C6 cells in which caveolin-1 was stably knocked-down by RNAi were transfected with $G\alpha_s$-GFP and imaged before agonist exposure (F) or after isoproterenol treatment at 15 min (G) and 30 min (H). I, $G\alpha_s$-GFP internalization in response to agonist was quantified by determining the mean fluorescence intensity in the cytoplasm of cells and is expressed as a percentage control. More than 50 cells in each treatment group were quantified from six or more independent experiments ($n = 6$). *, $p < 0.05$ versus CON. Scale bars, 10 μm (all panels).

βAR signaling and that cholesterol separates βARs from $G\alpha_s$, effectively dampening signaling. In C6 cells, adenylyl cyclase type VI is enriched in lipid rafts, and inhibition of AC by calcium influx is dependent on raft/caveolae integrity (Fagan et al., 2000). Forskolin-stimulated adenylyl cyclase activity is significantly increased after disrupting lipid rafts by depleting cholesterol (Rybin et al., 2000; Miura et al., 2001).

In previous reports, the roles of caveolae/rafts in regulating $G\alpha_s$/AC signaling have been implied from cholesterol chelation studies. This report provides the first evidence that genetic loss of caveolin-1 increases $G\alpha_s$/AC signaling in both a cell line and ex vivo from brain membranes. Our use of stable caveolin RNAi or caveolin-1 knockout to study GPCR/G_s/AC signaling is an important advance, because we can now clearly associate caveolin as a negative regulator of this pathway. Although cholesterol chelation studies remain a mainstay for disrupting cholesterol-enriched lipid microdomains, these techniques are less specific than molecular-based approaches. Because cholesterol influences membrane dynamics and also interacts with membrane proteins including the β_2AR (Hanson et al., 2008), we used the approach of genetic knockdown or knockout of caveolin. Although RNAi reduced caveolin protein by nearly 90%, membrane and total cholesterol levels were unchanged in the cells. This is a crucial observation because caveolins are cholesterol-binding proteins and are known to shuttle cholesterol from endoplasmic reticulm to plasma membrane (Smart et al., 1996). In addition, although a small level of caveolin-1 remains expressed after RNAi (~10%), it is unlikely that this has any effect because complete knockout of caveolin in brain membranes results in similar effects (Fig. 7). The novel result that loss of caveolin-1 in mice increases $G\alpha_s$/AC signaling in brain membranes (Fig. 7) suggests that caveolins dampen this signaling pathway in vivo, a finding that merits further study.

There are several theoretical mechanisms by which caveolins and rafts/caveolae might dampen $G\alpha_s$/AC signaling. One possibility is that caveolin knockdown prevents coupling between the βAR and $G\alpha_i$, which might increase cAMP accumulation by preventing $G\alpha_i$ inhibition of AC; however, this is unlikely, because pertussis toxin treatments of cells were without effect (Fig. 5). In addition, because AlF_4^-- and forskolin-stimulated AC activity is increased by caveolin-1 knockdown or knockout, the results suggest that noninvolvement of $G\alpha_i$ or a GPCR coupled to $G\alpha_i$. Alternatively, because caveolin-1 is a cholesterol-binding protein (Murata et al., 1995), limiting its expression could lower membrane cholesterol. This is not the case (Fig. 5). In fact, incubating wild-type or Cav-1 RNAi cells with 1 mg/ml exogenous cholesterol significantly decreased isoproterenol-stimulated cAMP accumulation (Fig. 5). Thus, removing membrane cholesterol does seem to enhance βAR/$G\alpha_s$/adenylyl cyclase signaling (most likely by disrupting rafts/caveolae), and adding cholesterol has the opposite effect. Therefore, the elevated cAMP signaling due to loss of caveolin is independent of $G\alpha_i$ and cholesterol levels.

Lipid rafts/caveolae can influence both spatial organization at the membrane and intracellular trafficking of signaling molecules; both mechanisms could regulate the $G\alpha_s$/adenylyl cyclase signaling cascade. Lipid rafts/caveolae could partition $G\alpha_s$

into lipid membrane domains, where it cannot effectively activate adenylyl cyclase (Willoughby and Cooper, 2007), or act as vehicles for $G\alpha_s$ internalization to remove $G\alpha_s$ from membrane signaling cascades (Allen et al., 2005). Either would result in attenuated GPCR signaling. Regarding partitioning and spatial organization in membrane microdomains, the fractionation data indicate approximately 70 to 80% of βARs, $G\alpha_s$, and AC are localized outside of caveolin-containing membrane fractions in *unstimulated* C6 cells (Fig. 2) (Allen et al., 2005). Not surprisingly, genetic loss of caveolin-1 decreases the level of $G\alpha_s$ and AC VI localized in raft/caveolae fractions, but this is probably due to a bulk decrease in formed caveolae (Fig. 2). The stoichiometry of βAR to $G\alpha_s$ in C6 cells is approximately 1:100 (Insel and Ostrom, 2003; Allen et al., 2005), suggesting that the majority of the βAR-$G\alpha_s$-AC coupling occurs outside of lipid rafts/caveolae in these cells. However, *during active signaling*, βARs are removed from lipid raft/caveolae domains, whereas $G\alpha_s$ significantly increases its localization in these domains (approximately 25% of total $G\alpha_s$ is in rafts/caveolae after agonist), suggesting that rafts/caveolae separate pools of the receptor and G protein during signaling (Rybin et al., 2000; Ostrom et al., 2001; Allen et al., 2005; Pontier et al., 2008). This dynamic shifting of the components into or out of microdomains during signaling likely contributes to both $G\alpha_s$ internalization (Fig. 6) and the ability to effectively constitute the AC signaling cascade.

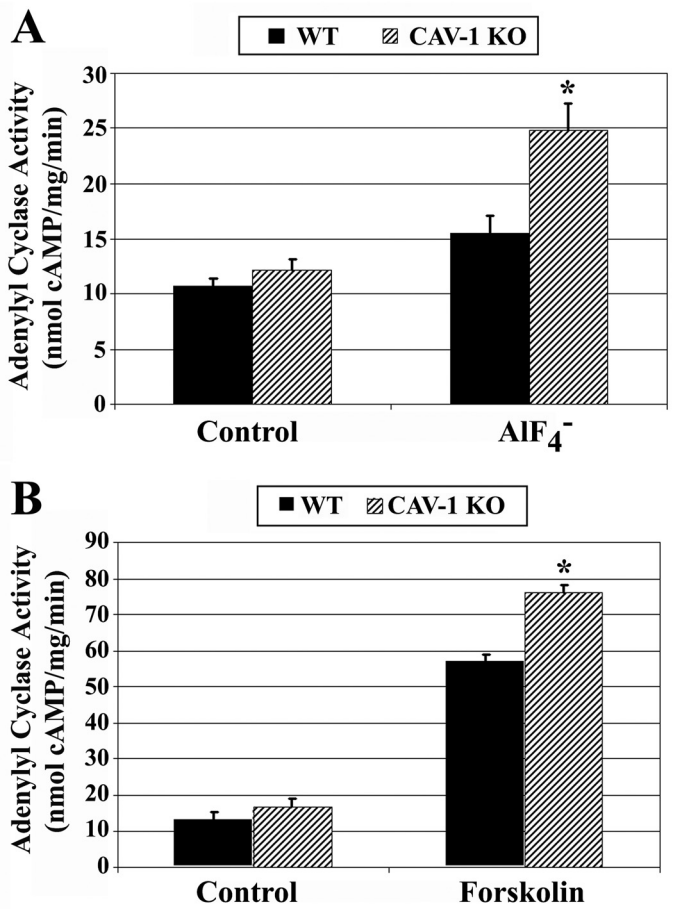

Fig. 7. Caveolin-1 knockout increases fluoride and forskolin-stimulated adenylyl cyclase activity in mouse striatum. Ten- to 12-week-old wild-type or caveolin-1 knockout littermate mice were colony bred, brains were obtained, and striatum was microdissected. 10 μg of isolated striatum membranes were assayed for adenylyl cyclase activity. A, striatum membranes from wild-type or caveolin-1 knockout mice were incubated for 20 min, with a reaction mixture including [^{32}P]ATP and ±10 mM sodium fluoride/20 μM aluminum chloride. [^{32}P]cAMP was isolated and determined by scintillation counting, normalized to time and milligrams of membrane protein. B, striatum membranes were incubated with ± 100 μM forskolin for 20 min [^{32}P]cAMP was isolated and determined by scintillation counting, normalized to time and milligrams of membrane protein. Data are the means ± S.E.M. from four littermate mice pairs ($n = 4$) assayed in triplicate. *, $p < 0.05$ versus wild-type mice for each treatment group.

Our previous studies investigating the trafficking of $G\alpha_s$-GFP estimate that approximately 50% of the total $G\alpha_s$ pool can be internalized during βAR signaling (Yu and Rasenick, 2002; Yu et al., 2009), and this internalization is completely blocked by disrupting lipid raft/caveolae endocytosis (Allen et al., 2005). The novel observation that caveolin knockdown prevents agonist-induced endocytosis of $G\alpha_s$ (Fig. 6) is likely to best explain the effects of elevated $G\alpha_s$/AC signaling (Fig. 3 and 4). These data suggest that during active signaling, lipid rafts/caveolae/caveolins promote endocytosis of activated $G\alpha_s$. Considering that a large pool of $G\alpha_s$ undergoes endocytosis during signaling and loss of caveolin prevents this trafficking, rafts/caveolae and caveolins would be anticipated to profoundly influence $G\alpha_s$/AC signaling.

This study also provides important new insights regarding the influence that caveolins and rafts/caveolae have on discreet GPCR-G protein signaling pathways. With respect to $G\alpha_s$ in this report, we find that caveolin knockdown greatly elevates $G\alpha_s$/AC signaling. In remarkable contrast, this same caveolin knockdown in C6 cells profoundly inhibits $G\alpha_q$-mediated signaling by the 5-HT_{2A} and P2Y receptors (Bhatnagar et al., 2004). This reveals that different receptors and G protein signaling pathways are differentially influenced by caveolins; $G\alpha_s$ signaling is inhibited, whereas $G\alpha_q$ is facilitated. Caveolins probably scaffold discreet molecular signaling elements and therefore control the functional actions of receptor pathways. Taken together, our studies predict that caveolins/rafts will regulate, differentially, the signals from many GPCRs at the level of the G protein.

There is also a complex relationship between $G\alpha_s$, lipid rafts, and the cytoskeleton that may be relevant to these data. $G\alpha_s$ binds to tubulin (Wang et al., 1990; Yu et al., 2009), and this binding seems to involve the region (switch III) of $G\alpha_s$ that interacts with effectors, such as adenylyl cyclase (Layden et al., 2008). Microtubule-disrupting drugs increase $G\alpha_s$ activation of AC (Rasenick et al., 1981), and this may be due to disruption of rafts/caveolae by these agents (Head et al., 2006). It is intriguing that long-term treatment with antidepressants increases $G\alpha_s$-AC coupling (Ozawa and Rasenick, 1989) and that this is associated with diminished localization of $G\alpha_s$ in lipid rafts (Donati and Rasenick, 2005). Finally, attenuated G_s/AC signaling in depression (Hines and Tabakoff, 2005) may be due to an increased proportion of $G\alpha_s$ being localized to lipid rafts, based on studies of brain tissue collected from depressed suicide victims (Donati et al., 2008). Thus, the interface between $G\alpha_s$, the cytoskeleton, and lipid rafts may represent a regulatory domain for hormone- and neurotransmitter action with relevance for mood disorders and drug response and responsiveness.

In summary, results from this study suggest that lipid rafts/caveolae and caveolins attenuate $G\alpha_s$/AC signaling. Stable caveolin knockdown or cyclodextrin treatments prevented agonist-induced internalization of $G\alpha_s$ and increased $G\alpha_s$/AC signaling. It is suggested that lipid rafts/caveolae are

sites that remove $G\alpha_s$ from membrane signaling cascades and also might globally dampen cAMP signaling, leading to a link between plasma membrane heterogeneity and hormone or neurotransmitter action.

Acknowledgments

We thank Dr. Debora Segaloff (University of Iowa, Iowa City, IA) for generously providing the human TSHR cDNA (Mizrachi and Segaloff, 2004). We thank Sadia Qureshi for excellent technical assistance. We thank AbdulRazzaq Al Siddiqi for his generous financial support of this project. We also thank members of the Rasenick laboratory for critical review and discussion of this manuscript.

References

Allen JA, Halverson-Tamboli RA, and Rasenick MM (2007) Lipid raft microdomains and neurotransmitter signalling. *Nat Rev Neurosci* **8:**128–140.

Allen JA, Yu JZ, Donati RJ, and Rasenick MM (2005) β-Adrenergic receptor stimulation promotes $G\alpha_s$ internalization through lipid rafts: a study in living cells. *Mol Pharmacol* **67:**1493–1504.

Bhatnagar A, Sheffler DJ, Kroeze WK, Compton-Toth B, and Roth BL (2004) Caveolin-1 interacts with 5-HT2A serotonin receptors and profoundly modulates the signaling of selected $G\alpha_q$-coupled protein receptors. *J Biol Chem* **279:**34614–34623.

Bradford MM (1976) A rapid and sensitive method for the quantitation of microgram quantities of protein utilizing the principle of protein-dye binding. *Anal Biochem* **72:**248–254.

Brown DA (2006) Lipid rafts, detergent-resistant membranes, and raft targeting signals. *Physiology* (*Bethesda*) **21:**430–439.

Cohen AW, Hnasko R, Schubert W, and Lisanti MP (2004) Role of caveolae and caveolins in health and disease. *Physiol Rev* **84:**1341–1379.

Daaka Y, Luttrell LM, and Lefkowitz RJ (1997) Switching of the coupling of the beta2-adrenergic receptor to different G proteins by protein kinase A. *Nature* **390:**88–91.

Debernardi MA, Munshi R, Yoshimura M, Cooper DM, and Brooker G (1993) Predominant expression of type-VI adenylate cyclase in C6–2B rat glioma cells may account for inhibition of cyclic AMP accumulation by calcium. *Biochem J* **293:**325–328.

Donati RJ, Dwivedi Y, Roberts RC, Conley RR, Pandey GN, and Rasenick MM (2008) Postmortem brain tissue of depressed suicides reveals increased G_s alpha localization in lipid raft domains where it is less likely to activate adenylyl cyclase. *J Neurosci* **28:**3042–3050.

Donati RJ and Rasenick MM (2005) Chronic antidepressant treatment prevents accumulation of gsalpha in cholesterol-rich, cytoskeletal-associated, plasma membrane domains (lipid rafts). *Neuropsychopharmacology* **30:**1238–1245.

Drab M, Verkade P, Elger M, Kasper M, Lohn M, Lauterbach B, Menne J, Lindschau C, Mende F, Luft FC, et al. (2001) Loss of caveolae, vascular dysfunction, and pulmonary defects in caveolin-1 gene-disrupted mice. *Science* **293:**2449–2452.

Evanko DS, Thiyagarajan MM, Siderovski DP, and Wedegaertner PB (2001) Gbeta gamma isoforms selectively rescue plasma membrane localization and palmitoylation of mutant Galphas and Galphaq. *J Biol Chem* **276:**23945–23953.

Fagan KA, Smith KE, and Cooper DM (2000) Regulation of the Ca^{2+}-inhibitable adenylyl cyclase type VI by capacitative Ca^{2+} entry requires localization in cholesterol-rich domains. *J Biol Chem* **275:**26530–26537.

Fra AM, Williamson E, Simons K, and Parton RG (1995) De novo formation of caveolae in lymphocytes by expression of VIP21-caveolin. *Proc Natl Acad Sci U S A* **92:**8655–8659.

Francesconi A, Kumari R, and Zukin RS (2009) Regulation of group I metabotropic glutamate receptor trafficking and signaling by the caveolar/lipid raft pathway. *J Neurosci* **29:**3590–3602.

Frank PG, Cheung MW, Pavlides S, Llaverias G, Park DS, and Lisanti MP (2006) Caveolin-1 and regulation of cellular cholesterol homeostasis. *Am J Physiol Heart Circ Physiol* **291:**H677–H686.

Hanson MA, Cherezov V, Griffith MT, Roth CB, Jaakola VP, Chien EY, Velasquez J, Kuhn P, and Stevens RC (2008) A specific cholesterol binding site is established by the 2.8 A structure of the human beta2-adrenergic receptor. *Structure* **16:**897–905.

Head BP, Patel HH, Roth DM, Lai NC, Niesman IR, Farquhar MG, and Insel PA (2005) G-protein-coupled receptor signaling components localize in both sarcolemmal and intracellular caveolin-3-associated microdomains in adult cardiac myocytes. *J Biol Chem* **280:**31036–31044.

Head BP, Patel HH, Roth DM, Murray F, Swaney JS, Niesman IR, Farquhar MG, and Insel PA (2006) Microtubules and actin microfilaments regulate lipid raft/caveolae localization of adenylyl cyclase signaling components. *J Biol Chem* **281:**26391–26399.

Hines LM, Tabakoff B, and WHO/ISBRA Study on State and Trait Markers of Alcohol Use and Dependence Investigators (2005) Platelet adenylyl cyclase activity: a biological marker for major depression and recent drug use. *Biol Psychiatry* **58:**955–962.

Hynes TR, Mervine SM, Yost EA, Sabo JL, and Berlot CH (2004) Live cell imaging of G_s and the beta2-adrenergic receptor demonstrates that both alphas and beta1gamma7 internalize upon stimulation and exhibit similar trafficking patterns that differ from that of the beta2-adrenergic receptor. *J Biol Chem* **279:**44101–44112.

Insel PA and Ostrom RS (2003) Forskolin as a tool for examining adenylyl cyclase expression, regulation, and G protein signaling. *Cell Mol Neurobiol* **23:**305–314.

Layden BT, Saengsawang W, Donati RJ, Yang S, Mulhearn DC, Johnson ME, and Rasenick MM (2008) Structural model of a complex between the heterotrimeric G protein, Gsalpha, and tubulin. *Biochim Biophys Acta* **1783:**964–973.

Le Roy C and Wrana JL (2005) Clathrin- and non-clathrin-mediated endocytic regulation of cell signalling. *Nat Rev Mol Cell Biol* **6:**112–126.

Levis MJ and Bourne HR (1992) Activation of the alpha subunit of G_s in intact cells alters its abundance, rate of degradation, and membrane avidity. *J Cell Biol* **119:**1297–1307.

Marrari Y, Crouthamel M, Irannejad R, and Wedegaertner PB (2007) Assembly and trafficking of heterotrimeric G proteins. *Biochemistry* **46:**7665–7677.

Miura Y, Hanada K, and Jones TL (2001) G(s) signaling is intact after disruption of lipid rafts. *Biochemistry* **40:**15418–15423.

Mizrachi D and Segaloff DL (2004) Intracellularly located misfolded glycoprotein hormone receptors associate with different chaperone proteins than their cognate wild-type receptors. *Mol Endocrinol* **18:**1768–1777.

Murata M, Peränen J, Schreiner R, Wieland F, Kurzchalia TV, and Simons K (1995) VIP21/caveolin is a cholesterol-binding protein. *Proc Natl Acad Sci U S A* **92:**10339–10343.

Oh P and Schnitzer JE (2001) Segregation of heterotrimeric G proteins in cell surface microdomains. G(q) binds caveolin to concentrate in caveolae, whereas G(i) and G(s) target lipid rafts by default. *Mol Biol Cell* **12:**685–698.

Ostrom RS, Gregorian C, Drenan RM, Xiang Y, Regan JW, and Insel PA (2001) Receptor number and caveolar co-localization determine receptor coupling efficiency to adenylyl cyclase. *J Biol Chem* **276:**42063–42069.

Ostrom RS and Insel PA (2004) The evolving role of lipid rafts and caveolae in G protein-coupled receptor signaling: implications for molecular pharmacology. *Br J Pharmacol* **143:**235–245.

Ozawa H and Rasenick MM (1989) Coupling of the stimulatory GTP-binding protein G_s to rat synaptic membrane adenylate cyclase is enhanced subsequent to chronic antidepressant treatment. *Mol Pharmacol* **36:**803–808.

Patel HH, Murray F, and Insel PA (2008) Caveolae as organizers of pharmacologically relevant signal transduction molecules. *Annu Rev Pharmacol Toxicol* **48:**359–391.

Pontier SM, Percherancier Y, Galandrin S, Breit A, Galés C, and Bouvier M (2008) Cholesterol-dependent separation of the β_2-adrenergic receptor from its partners determines signaling efficacy: insight into nanoscale organization of signal transduction. *J Biol Chem* **283:**24659–24672.

Rajendran L and Simons K (2005) Lipid rafts and membrane dynamics. *J Cell Sci* **118:**1099–1102.

Ransnäs LA, Svoboda P, Jasper JR, and Insel PA (1989) Stimulation of beta-adrenergic receptors of S49 lymphoma cells redistributes the alpha subunit of the stimulatory G protein between cytosol and membranes. *Proc Natl Acad Sci U S A* **86:**7900–7903.

Rasenick MM, Stein PJ, and Bitensky MW (1981) The regulatory subunit of adenylate cyclase interacts with cytoskeletal components. *Nature* **294:**560–562.

Rasenick MM, Wheeler GL, Bitensky MW, Kosack CM, Malina RL, and Stein PJ (1984) Photoaffinity identification of colchicine-solubilized regulatory subunit from rat brain adenylate cyclase. *J Neurochem* **43:**1447–1454.

Razani B, Engelman JA, Wang XB, Schubert W, Zhang XL, Marks CB, Macaluso F, Russell RG, Li M, Pestell RG, et al. (2001) Caveolin-1 null mice are viable but show evidence of hyperproliferative and vascular abnormalities. *J Biol Chem* **276:**38121–38138.

Rodbell M (1985) Programmable messengers: a new theory of hormone action. *Trends Biochem Sci* **10:**461–464.

Rybin VO, Xu X, Lisanti MP, and Steinberg SF (2000) Differential targeting of beta-adrenergic receptor subtypes and adenylyl cyclase to cardiomyocyte caveolae. A mechanism to functionally regulate the cAMP signaling pathway. *J Biol Chem* **275:**41447–41457.

Salomon Y (1979) Adenylate cyclase assay. *Adv Cyclic Nucleotide Res* **10:**35–55.

Smart EJ, Ying Y, Donzell WC, and Anderson RG (1996) A role for caveolin in transport of cholesterol from endoplasmic reticulum to plasma membrane. *J Biol Chem* **271:**29427–29435.

Sutkowski EM, Tang WJ, Broome CW, Robbins JD, and Seamon KB (1994) Regulation of forskolin interactions with type I, II, V, and VI adenylyl cyclases by G_s alpha. *Biochemistry* **33:**12852–12859.

Toki S, Donati RJ, and Rasenick MM (1999) Treatment of C6 glioma cells and rats with antidepressant drugs increases the detergent extraction of G_s alpha from plasma membrane. *J Neurochem* **73:**1114–1120.

Wang N, Yan K, and Rasenick MM (1990) Tubulin binds specifically to the signal-transducing proteins, G_s alpha and Gi alpha 1. *J Biol Chem* **265:**1239–1242.

Watts VJ and Neve KA (1996) Sensitization of endogenous and recombinant adenylate cyclase by activation of D2 dopamine receptors. *Mol Pharmacol* **50:**966–976.

Wedegaertner PB, Bourne HR, and von Zastrow M (1996) Activation-induced subcellular redistribution of G_s alpha. *Mol Biol Cell* **7:**1225–1233.

Willoughby D and Cooper DM (2007) Organization and Ca^{2+} regulation of adenylyl cyclases in cAMP microdomains. *Physiol Rev* **87:**965–1010.

Xiang Y, Rybin VO, Steinberg SF, and Kobilka B (2002) Caveolar localization dictates physiologic signaling of beta 2-adrenoceptors in neonatal cardiac myocytes. *J Biol Chem* **277:**34280–34286.

Yu JZ, Dave RH, Allen JA, Sarma T, and Rasenick MM (2009) Cytosolic $G\alpha_s$ acts as an intracellular messenger to increase microtubule dynamics and promote neurite outgrowth. *J Biol Chem* **284:**10462–10472.

Yu JZ and Rasenick MM (2002) Real-time visualization of a fluorescent $G\alpha_s$: dissociation of the activated G protein from plasma membrane. *Mol Pharmacol* **61:**352–359.

Address correspondence to: Dr. Mark M. Rasenick, Department of Physiology and Biophysics (MC 901), College of Medicine, University of Illinois at Chicago (UIC), 835 South Wolcott Avenue, Chicago, IL 60612-7342. E-mail: raz@uic.edu